NATIONAL ADVISORY COMMITTEE FOR AERONAUTICS

TECHNICAL MEMORANDUM 1375

ON THE THREE-DIMENSIONAL INSTABILITY OF LAMINAR

BOUNDARY LAYERS ON CONCAVE WALLS

By H. Görtler

Translation of "Über eine dreidimensionale Instabilität laminarer Grenzschichten an konkaven Wänden." Ges. d. Wiss. Göttingen, Nachr. a. d. Math., Bd. 2, Nr. 1, 1940.

NACA

Washington

June 1954

TECHNICAL MEMORANDUM 1375

ON THE THREE-DIMENSIONAL INSTABILITY OF LAMINAR

BOUNDARY LAYERS ON CONCAVE WALLS[*][1]

By H. Görtler

SUMMARY

The present report is a study of the stability of laminar boundary-layer profiles on slightly curved walls relative to small disturbances, in the shape of vortices, whose axes are parallel to the principal direction of flow. The result in an eigenvalue problem by which, for a given undisturbed flow at a prescribed wall, the amplification or decay is computed for each Reynolds number and each vortex thickness. For neutral disturbances (amplification null) a critical Reynolds number is determined for each vortex distribution. The numerical calculation produces amplified disturbances on concave walls only. The variation of the dimensionless $\dfrac{U_0 \vartheta}{\nu}\sqrt{\dfrac{\vartheta}{R}}$ with respect to $\alpha\vartheta$ is only slightly dependent on the shape of the boundary-layer profile. The numerical results yield information about stability limit, range of wave length of vortices that can be amplified, and about the most dangerous vortices with regard to the transition from laminar to turbulent flow. At the very first appearance of amplified vortices the flow still is entirely regular; transition to turbulent flow may not be expected until the Reynolds numbers are higher.

1. INTRODUCTION

Until now the stability calculations of laminar two-dimensional fluid flows on straight walls had usually been based upon disturbances in the shape of plane wave motions which travel in the direction of the flow. After some initial failures (see Noether's comprehensive report, 1921 (ref. 2)), the researches by Prandtl, Tietjens, Tollmien, and Schlichting

---

[*]"Über eine dreidimensionale Instabilität laminarer Grenzschichten an konkaven Wänden." Ges. d. Wiss. Göttingen, Nachr. a. d. Math., Bd. 2, Nr. 1, 1940.

[1]Presents part of a thesis by H. Görtler submitted in partial fulfillment of the requirements for the degree of Dr. Phil. in Math - Natural Sciences Faculty of the University of Göttingen.

have, since 1921, produced results which compared well with observations
and to a certain extent yielded information about the important question
of the origin of turbulence from small disturbances. Schlichting, 1934
(ref. 7), gave a report on the results of these investigations. A brief
glance at the method is indicated.

In these calculations, a velocity distribution $U(y)$ that depends
only on the coordinate y at right angles to the plane of the wall is
assumed as the basic flow. The omission of variations of the laminar
basic flow in the x-direction (= principal flow direction parallel to
wall) was dictated by mathematical reasons; and the results of the calcu-
lations enabled valuable deductions to be made as long as the variations
in x-direction were not excessive. To the basic flow $U(y)$ were added
disturbances of assumedly sufficient smallness to permit linearization of
the hydrodynamic equations with regard to the components of the disturb-
ance. This way the problem could be narrowed down to an expression for
the stream function of the disturbance in the form

$$\psi(x,y,t) = \varphi(y)e^{i(\alpha x - \beta t)} \tag{1.1}$$

A particular disturbance can then be built up by the Fourier method as a
disturbance of a general kind by a linear combination of such partial
oscillations. While α is assumed as real, the prefix of the imaginary
part of β determines whether there is amplification or damping with
increasing time t.

The more general expression of three-dimensional disturbances in the
form of traveling waves, which are parallel to the flat wall but oblique
to the base flow direction, hence, for which the velocity compo-
nents $u_i(i = 1,2,3)$ are given by

$$u_i = f_i(y)e^{i(\alpha_1 x + \alpha_2 z - \beta t)} \tag{1.2}$$

(z coordinate parallel to wall and perpendicular to principal flow direc-
tion), was analyzed by H. B. Squire (ref. 6). By comparison with the
aforementioned special case (1.1) to be treated independently, he was able
to show that, in the case of the disturbances (1.2) with $\alpha_1 \neq 0$, $\alpha_2 \neq 0$,
amplification always occurrs at higher Reynolds numbers than in the case
of the disturbances (1.1) with $\alpha^2 = \alpha_1^2 + \alpha_2^2$. Therefore, the investi-
gation can be limited to two-dimensional disturbances of the form (1.1).

The stability investigation of laminar boundary layers relative to
these disturbances was also applied to curved walls (x is then the arc
length of the wall). Tollmien's claculations for the flat plate with
allowance for friction were applied by Schlichting (ref. 5) to the case

of flow within a rotating circular cylinder. The stabilizing effect of
the wall curvature is such that the critical Reynolds number, formed with
the displacement thickness $\delta*$ of the boundary layer, increases with
increasing $\delta*/R$ (R = radius of circular cylinder). This stabilizing
effect corresponds likewise with the concepts associated with the action
of the centrifugal force (compare Prandtl, ref. 4).

Boundary-layer flows on slightly curved stationary walls were inves-
tigated by the writer (ref. 10) for stability against two-dimensional dis-
turbances of the form (1.1). Tollmien's result for flat walls, with fric-
tion neglected and, hence, with the evaluation of the critical Reynolds
number disregarded, was the well-known stability criterion which states
that boundary-layer profiles with inflection point are unstable. Such
profiles are characterized by a pressure rise from the outside of the
boundary layer in the direction of flow. For curved walls, this criterion
is modified to the extent that, instead of the stipulated change of the
sign of $U''(y)$, a change of sign at $U'' + \frac{1}{R} U'$ is necessary (curvature
radius R of wall positive on walls convex to flow, negative on walls
concave to flow). This Tollmien instability occurs, therefore, on concave
walls only after the minimum of the pressure impressed on the boundary
layer from without, and on convex walls already before the pressure mini-
mum. However, the effect of the wall curvature is extremely small.

It is surprising that convex stationary walls in this sense act
amplifying, but concave walls stabilizing, hence, that the effect of the
centrifugal force does not appear. A confirmation of the criterion fol-
lows from the fact that the same can be applied also to Schlichting's
case of a rotating cylinder, as explained in detail in the aforementioned
report. There the criterion, in accord with Schlichting's results, yields
a stabilizing effect of the rotating concave wall. In unpublished calcu-
lations, Schlichting investigated the case of the stationary curved wall
in analogy to his own and Tollmien's calculations for the flat wall, with
allowance for friction, for the purpose of observing the wall-curvature
effect on the critical Reynolds number. In a personal conversation,
Mr. Schlichting told me that these calculations also proved the stabi-
lizing effect of concave walls and amplifying effect of convex walls.

In the present report, it will be shown that boundary-layer profiles
on concave walls can become unstable relative to certain three-dimensional
disturbances. It involves an instability that does not occur on flat or
convex walls. The friction is duly allowed for in the calculations and
even the impediment due to the now more complicated type of disturbance
can be overcome in a relatively simple manner. As to the type of these
disturbances, they are similar to those investigated by Taylor in 1923
(ref. 3) in the flow between rotating cylinders and which led to the well-
known instability (excellently confirmed by experiments Taylor made at the
same time) in the form of appearance of sharply defined vortices distrib-
uted boxlike in rectangular zones (compare fig. 1) taken from Taylor's
report.

The expression of corresponding equidistant vortices in the boundary layer at a curved wall, in which the axes of the vortices are parallel to the principal flow direction (see representation in fig. 2), leads through the Navier-Stokes equations and the equation of continuity to an eigenvalue problem: The amplification of the vortex disturbance for a prescribed basic flow on a given wall must be computed for each vortex disturbance and each Reynolds number of the basic flow; in particular for the neutral disturbances (zero amplification) a "critical Reynolds number" for each vortex distance must be determined. It is interesting to know how these results tie in with the type of basic flow and the wall curvature, and also the size of the vortices which are amplified first at increasing Reynolds number, as well as the question of the most dangerous vortices from the point of view of transition from laminar to turbulent flow.

At the present state of the experimental investigations, only the order of magnitude of the effect is of interest. All the calculations are centered on these claims, hence do not aim at an exhaustive mathematical treatment of the present disturbance problem but rather to a reply to the questions of interest in practice with an expenditure justifiable to the claim.

2. DEVELOPMENT OF THE DIFFERENTIAL EQUATIONS OF DISTURBANCE

Consider the case of two-dimensional flow of a viscous fluid on a slightly curved stationary wall. The finite curvature radius R of the wall is, for the sake of simplicity, assumed as constant, and R is assumed great compared to the boundary-layer thickness δ on the wall formed under the influence of the viscosity; R is chosen positive for walls concave to the flow - since the instability to be explored occurs only on concave walls - and negative for walls convex to the flow.

The basic flow is along the x-direction (x = arc length along the wall), $y(\geq 0)$ is the vertical wall distance, and z is the coordinate at right angle to both in the direction of the cylinder axis out of whose surface portion the wall is formed.

In these coordinates, the first Navier-Stokes equation, for example, reads in full rigor and generality

$$\frac{\partial u}{\partial t} + \frac{R}{R-y} u \frac{\partial u}{\partial x} + v \frac{\partial u}{\partial y} - \frac{uv}{R-y} + w \frac{\partial u}{\partial z} =$$

$$- \frac{R}{R-y} \frac{1}{\rho} \frac{\partial p}{\partial x} + \nu \left\{ \frac{R^2}{(R-y)^2} \frac{\partial^2 u}{\partial x^2} + \frac{\partial^2 u}{\partial y^2} + \frac{\partial^2 u}{\partial z^2} - \right.$$

$$\left. \frac{1}{R-y} \frac{\partial u}{\partial y} - \frac{2R}{(R-y)^2} \frac{\partial v}{\partial x} - \frac{u}{(R-y)^2} \right\}$$

where u, v, w are the velocity components of the total flow in x-, y-, and z-directions, p the pressure, ρ the density, and ν the kinematic viscosity of the flowing medium. All flow variations in x-direction are disregarded as customary, and R is assumed great with respect to δ by binomial development of $\frac{1}{R-y}$ and $\frac{1}{(R-y)^2}$. The Navier-Stokes equations and the continuity equation, up to the terms of the order $\frac{\delta}{R}$, read then

$$\left.\begin{array}{l} \dfrac{\partial u}{\partial t} + v\left(\dfrac{\partial u}{\partial y} - \dfrac{u}{R} \right) + w \dfrac{\partial u}{\partial z} = \nu\left(\dfrac{\partial^2 u}{\partial y^2} + \dfrac{\partial^2 u}{\partial z^2} - \dfrac{1}{R} \dfrac{\partial u}{\partial y} \right) \\[3mm] \dfrac{\partial v}{\partial t} + v \dfrac{\partial v}{\partial y} + \dfrac{u^2}{R} + w \dfrac{\partial v}{\partial z} = - \dfrac{1}{\rho} \dfrac{\partial p}{\partial y} + \nu\left(\dfrac{\partial^2 v}{\partial y^2} + \dfrac{\partial^2 v}{\partial z^2} - \dfrac{1}{R} \dfrac{\partial v}{\partial y} \right) \\[3mm] \dfrac{\partial w}{\partial t} + v \dfrac{\partial w}{\partial y} + w \dfrac{\partial w}{\partial z} = - \dfrac{1}{\rho} \dfrac{\partial p}{\partial z} + \nu\left(\dfrac{\partial^2 w}{\partial y^2} + \dfrac{\partial^2 w}{\partial z^2} - \dfrac{1}{R} \dfrac{\partial w}{\partial y} \right) \\[3mm] \dfrac{\partial v}{\partial y} - \dfrac{v}{R} + \dfrac{\partial w}{\partial z} = 0 \end{array}\right\} \quad (2.1)$$

The undisturbed flow $u = u_0(y,t)$, $v = 0$, $w = 0$, $p = p_0$, which itself is to be a solution of the hydrodynamic equations, for which, therefore,

$$\frac{\partial u_0}{\partial t} = v \frac{\partial^2 u_0}{\partial y^2} - \frac{1}{R} \frac{\partial u_0}{\partial y}$$

$$\frac{u_0^2}{R} = - \frac{1}{\rho} \frac{\partial p_0}{\partial y}$$

are applicable, is to change very little during the interval in which the disturbances are to be observed. Therefore, $\frac{\partial u_0}{\partial t}$ and, hence, its equivalent viscosity term is deliberately disregarded hereafter and u_0 is put $= u_0(y)$.

This basic flow $u_0(y)$ is a laminar boundary-layer flow formed by some previous history based on the viscosity effect. Use is made occasionally of the conventional idealization of such a boundary layer, which consists in assuming instead of the asymptotic transition in the outer flow $u_0 = U_0 =$ const., an increase of $u_0(0) = 0$ at the wall up to the value $u_0(\delta) = U_0$ at a certain point $y = \delta =$ "boundary-layer thickness," while putting $u_0 = U_0$ for $y \geqq \delta$. The minor effect of the assumedly slight wall curvature on the outside flow is ignored, since it plays no part within the framework of our theory of a first approximation.

On the assumption that $R \gg \delta$, the term $\frac{-u}{R}$ relative to $\frac{\partial u}{\partial y}$ and the term $- \frac{1}{R} \frac{\partial u}{\partial y}$ with respect to $\frac{\partial^2 u}{\partial y^2}$ can be disregarded in the equations (2.1) on account of $\frac{\partial u}{\partial y} \sim \frac{u}{\delta}$, $\frac{\partial^2 u}{\partial y^2} \sim \frac{1}{\delta} \frac{\partial u}{\partial y}$. The same applies to the two other velocity components. The essential effect of the wall curvature becomes evident in the term $\frac{u^2}{R}$ of the second equation (2.1). Moreover, no systematic difficulties are encountered if the cited small terms are carried along in the subsequent calculation. But, since they only hamper the task and contribute nothing to the effect involved, they are discounted.

So, in conformity with the arrangements at the beginning, the following disturbance equation is used:

$$
\left.
\begin{array}{l}
u = u_0(y) + u_1(y) \, \cos \, \alpha z e^{\beta t} \\[4pt]
v = v_1(y) \, \cos \, \alpha z e^{\beta t} \\[4pt]
w = w_1(y) \, \sin \, \alpha z e^{\beta t} \\[4pt]
p = p_0(y) + p_1(y) \, \cos \, \alpha z e^{\beta t}
\end{array}
\right\} \qquad (2.2)
$$

α is to be real and the calculation for β itself is to result in real values; $\alpha = \dfrac{2\pi}{\lambda}$, where λ is the wave length of the disturbance. The quantity β governs the amplification or damping of the flow, depending upon whether it is greater or smaller than zero. The equation (2.2) corresponds to a vortex distribution at the curved wall, the axes of which coincide with the direction of the principal flow. Figure 5 represents the streamline pattern in a section normal to the principal flow direction.

Introduction of equation (2.2) in the equations (2.1) following the omissions arising from $R \gg \delta$ results in the linearized equations with respect to the disturbance

$$
\beta u_1 + v_1 \, \frac{du_0}{dy} = \nu \left(\frac{d^2 u_1}{dy^2} - \alpha^2 u_1 \right) \qquad (2.3.1)
$$

$$
\beta v_1 + u_1 \, \frac{2u_0}{R} + \frac{1}{\rho} \, \frac{dp_1}{dy} = \nu \left(\frac{d^2 v_1}{dy^2} - \alpha^2 v_1 \right) \qquad (2.3.2)
$$

$$
\beta w_1 - \frac{\alpha}{\rho} \, p_1 = \nu \left(\frac{d^2 w_1}{dy^2} - \alpha^2 w_1 \right) \qquad (2.3.3)
$$

$$
w_1 = - \frac{1}{\alpha} \, \frac{dv_1}{dy} \qquad (2.3.4)
$$

They apply as long as the disturbance velocities are small with respect to the basic-flow velocity.

To treat this system of ordinary differential equations for the unknown functions u_1, v_1, w_1, and p_1, we insert w_1 from (2.3.4) in (2.3.3). The result is p_1 as a differential expression of the third

order in v_1. On substituting this expression for p_1 in (2.3.2), u_1 appears as differential expression of the fourth order in v_1. Combined with (2.3.1), the following system of coupled differential equations is obtained for u_1 and v_1:

$$\nu \frac{d^2 u_1}{dy^2} - (\beta + \nu\alpha^2) \, u_1 = v_1 \frac{du_0}{dy} \qquad (2.4.1)$$

$$\nu \frac{d^4 v_1}{dy^4} - (\beta + 2\nu\alpha^2) \frac{d^2 v_1}{dy^2} + \alpha^2(\beta + \nu\alpha^2)v_1 = - \frac{2\alpha^2 u_0}{R} u_1 \quad (2.4.2)$$

When u_1 and v_1 are known, w_1 and p_1 are computed from (2.3.4) and (2.3.3).

It is not recommended to set up a differential equation of the sixth order for u_1 or for v_1 alone by further elimination. The subsequent calculations are rather based direct on the systems (2.4.1) and (2.4.2) and merely produce a simplified mode of writing. With δ denoting a suitably chosen measure for the boundary-layer thickness, the following dimensionless factors are utilized:

$$\left.\begin{array}{l} \eta = \dfrac{y}{\delta} \\[2ex] \sigma = \alpha\delta \\[2ex] \mu = 2\left(\dfrac{U_0\delta}{\nu}\right)^2 \dfrac{\delta}{R} \\[2ex] U = \dfrac{u_0}{U_0} \\[2ex] \tau = \sqrt{\alpha^2\delta^2 + \dfrac{\beta\delta^2}{\nu}} \end{array}\right\} \qquad (2.5)$$

For neutral disturbances, that is, that state of transition in which the disturbances are neither amplified nor damped, $\beta = 0$, hence $\tau = \sigma$.

It further is appropriate to use the quantities

$$u' = \left(\frac{U_0 \delta}{\nu}\right)^{-1} u_1 \left.\begin{array}{c} \\ \\ \end{array}\right\}$$

$$v' = v_1$$

$$(2.6)$$

instead of u_1 and v_1. The prime is also omitted in the following without running a chance of causing a mixup with u and v defined by (2.2).

The differential equations (2.4.1) and (2.4.2) can be written briefly as differential equations for u and v, as follows:

$$Lu = \frac{dU}{d\eta} v \left.\begin{array}{c} \\ \\ \end{array}\right\}$$

$$L_0 Lv = -\sigma^2 \mu U u$$

$$(2.7)$$

by utilizing the differential operators

$$L = \frac{d^2}{d\eta^2} - \tau^2$$

$$L_0 = \frac{d^2}{d\eta^2} - \sigma^2$$

In conformity with the order of this system, six boundary conditions can be prescribed. It is especially stipulated that $u_1(0) = v_1(0) = w_1(0) = 0$, i.e., that the fluid hugs the wall. So with consideration to (2.3.4), it is required that $u(0) = v(0) = v'(0) = 0$. With the other three conditions, the decay of the disturbance at $\eta \longrightarrow \infty$ is attainable, or when the boundary layer at $y = \delta$, that is, $\eta = 1$ is permitted to change to the constant outside flow. Thus the smooth junction of three disturbance components with the respective values decaying with $\eta \longrightarrow \infty$ outside the boundary layer is assured. The symbol "∞" signifies "sufficiently great."

The homogeneous system of differential equations (2.7) together with six homogeneous boundary conditions produce an eignevalue problem for the

proposed values of $U(\eta)$ and R/δ: The magnitude of amplification β for every given wave length λ and every given Reynolds number $Re = \dfrac{U_0 \delta}{\nu}$ must be determined (i.e., the relationship existing between the parameters τ, σ, and μ, required for solving the homogeneous boundary value problem, must be calculated). The neutral disturbances ($\beta = 0$, that is, $\tau = \sigma$) especially, call for the determination of a "critical" Reynolds number of every wave length of disturbance λ, at which the particular disturbance is exactly maintained without amplifying or decaying.

In the subsequent analysis of the eigenvalue, the practical aspect is the primary object—namely, at what Reynolds number does amplification appear (stability limit)? What is the range of the wave lengths of disturbances that can be amplified at all? At what wave lengths does amplification appear first when Re increases? What disturbances are amplified most and are therefore most dangerous from the point of view of turbulence? What effect has the amount of the wall curvature on these data? Are there appreciable differences when different boundary-layer profiles $U(\eta)$ are used as basis? The question of calculating the eigenfunction is disregarded in the present report, although it may be stated that the method developed enables an approximate representation of it.

It is readily apparent from (2.7) that the Reynolds number and the wall curvature appear only in the form of the dimensionless $\dfrac{U_0 \delta}{\nu} \sqrt{\dfrac{\delta}{R}}$ (namely, in parameter μ).

3. CONVERSION OF THE DIFFERENTIAL EQUATIONS OF DISTURBANCE

TO AN EQUIVALENT SYSTEM OF INTEGRAL EQUATIONS

Green's function $G\left(\eta; \eta_0\right)$ is identified by the following postulates:

(1) $G\left(\eta; \eta_0\right)$ in $0 \leqq \eta \leqq \infty$ at $\eta \neq \eta_0$ is twice differentiable with respect to η.

(2) $LG \equiv \dfrac{d^2 G}{d\eta^2} - \tau^2 G = 0$ at $\eta \neq \eta_0$ in $0 \leqq \eta \leqq \infty$.

(3) $G\left(\eta; \eta_0\right)$ is continuous at the point $\eta = \eta_0$, but has in its first derivative the discontinuity defined by

$$\lim_{\epsilon \to 0} \left\{ \frac{dG}{d\eta}\left(\eta_0 + \epsilon; \eta_0\right) - \frac{dG}{d\eta}\left(\eta_0 - \epsilon; \eta_0\right) \right\} = -1$$

(4) $G\left(0; \eta_0\right) = 0$ and G also disappears at $\eta \to \infty$.

Green's function $H(\eta; \eta_0)$ is to have the following quality:

(1) $H(\eta; \eta_0)$ is four times continuously differentiable with respect to η in $0 \leqq \eta \leqq \infty$ at $\eta \neq \eta_0$.

(2) $L_0 L H = 0$ at $\eta \neq \eta_0$ in $0 \leqq \eta \leqq \infty$.

(3) At the point $\eta = \eta_0$, $H(\eta; \eta_0)$ is continuous including first and second derivatives, but the third derivative has the discontinuity

$$\lim_{\epsilon \longrightarrow 0} \left\{ \frac{d^3 H}{d\eta^3} \left(\eta_0 + \epsilon; \eta_0 \right) - \frac{d^3 H}{d\eta^3} \left(\eta_0 - \epsilon; \eta_0 \right) \right\} = -1$$

(4) $H(0; \eta_0) = \frac{dH}{d\eta} (0; \eta_0) = 0$ and H disappears at $\eta \longrightarrow \infty$.

By these requirements, G and H at $0 \leqq \eta \leqq \infty$ are clearly identified. The calculation gives

$$G(\eta; \eta_0) = \begin{cases} \dfrac{1}{\tau} e^{-\tau\eta_0} \sinh \tau\eta & \text{for } \eta \leqq \eta_0 \\[2ex] \dfrac{1}{\tau} e^{-\tau\eta} \sinh \tau\eta_0 & \text{for } \eta_0 \leqq \eta \end{cases}$$

$$H(\eta; \eta_0) = \begin{cases} \dfrac{1}{(\sigma + \tau)(\sigma - \tau)^2} \left[\left(e^{-\sigma\eta_0} - e^{-\tau\eta_0} \right) \left(\cosh \sigma\eta - \cosh \tau\eta \right) \right. \\[2ex] \left. - \dfrac{1}{\sigma\tau} \left(\tau e^{-\sigma\eta_0} - \sigma e^{-\tau\eta_0} \right) \left(\tau \sinh \sigma\eta - \sigma \sinh \tau\eta \right) \right] \quad \text{for } \eta \leqq \eta_0 \\[3ex] \dfrac{1}{(\sigma + \tau)(\sigma - \tau)^2} \left[\left(e^{-\sigma\eta} - e^{-\tau\eta} \right) \left(\cosh \sigma\eta_0 - \cosh \tau\eta_0 \right) \right. \\[2ex] \left. - \dfrac{1}{\sigma\tau} \left(\tau e^{-\sigma\eta} - \sigma e^{-\tau\eta} \right) \left(\tau \sinh \sigma\eta_0 - \sigma \sinh \tau\eta_0 \right) \right] \quad \text{for } \eta_0 \leqq \eta \end{cases}$$

$$(3.1)$$

In the event that $\beta = 0$, $H\left(\eta; \eta_0\right)$ becomes

$$
H\left(\eta; \eta_0\right) = \begin{cases} \dfrac{1}{4\sigma^3}\left[e^{-\sigma\left(\eta_0 + \eta\right)}\left\{2\sigma^2\eta_0\eta + \sigma\left(\eta_0 + \eta\right) + 1\right\} - \right. \\[2ex] \left. e^{-\sigma\left(\eta_0 - \eta\right)}\left\{\sigma\left(\eta_0 - \eta\right) + 1\right\}\right] \qquad \text{for } \eta \leqq \eta_0 \\[3ex] \dfrac{1}{4\sigma^3}\left[e^{-\sigma\left(\eta + \eta_0\right)}\left\{2\sigma^2\eta\eta_0 + \sigma\left(\eta + \eta_0\right) + 1\right\} - \right. \\[2ex] \left. e^{-\sigma\left(\eta - \eta_0\right)}\left\{\sigma\left(\eta - \eta_0\right) + 1\right\}\right] \qquad \text{for } \eta_0 \leqq \eta \end{cases} \tag{3.1a}
$$

The differential equation system (2.7) is equivalent to the integral equation system

$$
\left.\begin{aligned} u(\eta) &= -\int_0^\infty G\left(\eta; \eta_0\right) \frac{dU\left(\eta_0\right)}{d\eta_0} v\left(\eta_0\right)d\eta_0 \\[2ex] v(\eta) &= \sigma^2\mu \int_0^\infty H\left(\eta; \eta_0\right) U\left(\eta_0\right)u\left(\eta_0\right)d\eta_0 \end{aligned}\right\} \tag{3.2}
$$

4. METHOD OF DEFINING THE EIGENVALUES

To begin with, the integration interval is divided into partial intervals of the same length d, and $\eta_0^{(k)}$ and $\eta^{(k)}$ signify points of the k-th partial interval: $(k - 1) d \leqq \eta_0^{(k)} \leqq kd$ $(k = 1, 2, 3...)$, and where, for simplicity sake, $\eta^{(k)} = \eta_0^{(k)}$. The subscript k added to a function symbol indicates that the particular function is to be formed at a point of the k-th partial interval, say about $U_k = U\left(\eta_0^{(k)}\right)$; furthermore, $G_{ik} = G\left(\eta^{(i)}; \eta_0^{(k)}\right)$, $H_{ik} = H\left(\eta^{(i)}; \eta_0^{(k)}\right)$. By reason of the symmetry of the Green functions, $G_{ik} = G_{ki}$ and $H_{ik} = H_{ki}$.

Patterned after the Fredholm theory the integral in (3.2) is replaced by summation

$$u_i = -d \sum_{k=1}^{\infty} G_{ik} U_k{}' v_k \qquad (4.1a)$$

$$(i = 1,2,3,\ldots)$$

$$v_i = \sigma^2 \mu d \sum_{k=1}^{\infty} H_{ik} U_k u_k \qquad (4.1b)$$

$U_k{}'$ disappears for sufficiently great arguments $\eta_0{}^{(k)}$. Letting, as approximation to the asymptotic transition, the boundary layer change to $U = $ Constant at $\eta = 1$ (that is, $y = \delta$), it can be stated more accurately that $U_k{}' = 0$ at $\eta_0{}^{(k)} \geqq 1$. Thus at finite d a finite sum is involved in the summation (4.1a). If $nd = 1$, the summation along k must be extended from 1 to n. As a result, only the v_k with $k \leqq n$ appear on the right-hand side of the equation (4.1a).

Correspondingly, considering only the equations with the v_i at which $i \leqq n$ in (4.1b), the infinite sum on the right-hand side can be approximately replaced by a finite sum of $k - 1$ up to a sufficiently great $k = N$, because the values H_{ik} decrease rapidly with increasing k owing to the upwardly restricted $i \leq n$ (the u_k themselves decay with increasing k). The homogeneous system of the $n + N$ equations is therefore investigated

$$\left.\begin{aligned} u_i + d \sum_{k=1}^{n} G_{ik} U_k{}' v_k = 0 \qquad (i = 1,2,\ldots,N) \\[2em] \sigma^2 \mu d \sum_{k=1}^{N} H_{ik} U_k u_k - v_i = 0 \qquad (i = 1,2,\ldots,n) \end{aligned}\right\} \qquad (4.2)$$

for the N unknown $u_i (i = 1,2,\ldots N)$ and the n unknown $v_i (i = 1,2,\ldots n)$.

The vanishing of the determinants

$$
\begin{vmatrix}
1 & 0 & \cdots & 0 & G_{11}U_1{}'d & G_{12}U_2{}'d & \cdots & G_{1n}U_n{}'d \\
0 & 1 & \cdots & 0 & G_{21}U_1{}'d & G_{22}U_2{}'d & \cdots & G_{2n}U_n{}'d \\
\cdots & \cdots & \cdots & \cdots & \cdots & \cdots & \cdots & \cdots \\
0 & 0 & \cdots & 1 & G_{N1}U_1{}'d & G_{N2}U_2{}'d & \cdots & G_{Nn}U_n{}'d \\
\sigma^2\mu H_{11}U_1 d & \sigma^2\mu H_{12}U_2 d & \cdots & \sigma^2\mu H_{1N}U_N d & -1 & 0 & & 0 \\
\sigma^2\mu H_{21}U_1 d & \sigma^2\mu H_{22}U_2 d & \cdots & \sigma^2\mu H_{2N}U_N d & 0 & -1 & \cdots & 0 \\
\cdots & \cdots & \cdots & \cdots & \cdots & \cdots & \cdots & \cdots \\
\sigma^2\mu H_{n1}U_1 d & \sigma^2\mu H_{n2}U_2 d & \cdots & \sigma^2\mu H_{nN}U_N d & 0 & 0 & \cdots & -1
\end{vmatrix}
$$

$$(4.3)$$

postulated for the existance of a nontrivial solution system leaves an algebraic equation for μ at given U, σ, and τ and, especially, the critical value of the dimensionless $\dfrac{U_0\delta}{\nu}\sqrt{\dfrac{\delta}{R}}$ for $\tau = \sigma$.

Every point $\eta^{(k)}$ within the boundary layer contributes two nontrivial series to the determinant—that is, two series (or gaps) in which not only the terms of the principal diagonal are different from zero; a point at the border or outside of the boundary layer supplies only a nontrivial series; the wall point (say, chosen as $\eta^{(1)}$) produces only trivial series because there the Green functions (and U also) disappear.

5. CALCULATION OF CRITICAL REYNOLDS NUMBER VARIATION

IN ITS MINIMUM WAVE LENGTH RANGE

A few words concerning the choice of basic flow for the proposed numerical calculations are indicated. Theoretically, the basic flow U represents any boundary-layer flow formed at a wall due to friction and some earlier history. The present calculations are based on the data of the Blasius boundary layer of the flat plate (ref. 8). Several other profile forms are included for comparison.

As regards the profile U of the plate boundary layer, the wall distance at which the boundary layer in its asymptotic transition to the outside flow diverges only 1 percent from this flow (curve 1, fig. 5) serves as measure δ for the boundary-layer thickness. This is the wall distance at which the variable $\dfrac{y}{2}\sqrt{\dfrac{U_0}{\nu x}}$ in Blasius's report assumes the value 3.

As a practical check on the quality of convergence of the calculation method developed in section 4, $\eta^{(k)} = \eta_0(k) = \dfrac{k-1}{n}$ and $d = \dfrac{1}{n}$ were selected and the following three approximations calculated: for $\eta^{(k)}$ and $\eta_0(k)$, the points 0, 1/2, 1; 0, 1/3, 2/3, 1; 0, 1/4, 1/2, 3/4, 1 were taken. According to the remarks made at the conclusion of the preceding section 4, the calculation of three-, five-, or seven-row determinants is involved, which result in a linear or quadratic or cubic equation for μ with respect to σ and τ. Evaluation for neutral disturbances ($\tau = \sigma$) showed that, to each value of the parameter $\sigma = \alpha\delta$, that is, to each wave length of disturbance there corresponds the related value of μ as smallest root. Since the equations exhibit, on the whole, coefficients with alternating prefix, only positive roots μ are obtained by this calculation, that is, positive values of the critical dimensionless $\left(\dfrac{U_0\delta}{\nu}\right)^2 \dfrac{\delta}{R}$, hence an instability of the assumed type only on concave walls $(R > 0)$ result.

The results of this preliminary calculation are shown in figure 4. The convergence for the parts of the curve above greater or smaller $\alpha\delta$ values, where the curves continue to rise, was not quite satisfactory. But the range of the minimum, which is of chief interest here, emerges sufficiently accurate.

Beyond these approximations, other points $\eta^{(k)}$ outside the boundary layer were assumed for individual $\alpha\delta$ values as a check that the approximations achieved in figure 4 are not subjected to appreciable changes. The minimum becomes a few percent less and shifts slightly toward smaller $\alpha\delta$ values.

Incidentally, it should be noted that the order of magnitude of these numerical values had been checked by special calculations. Originally it had been attempted to solve (2.7) by expanding η in power series. The convergence for u and v from $\eta = 0$ on was very slow. Therefore, series from $\eta = 1$ on were resorted to. Corresponding to the order of the differential-equation system and the number of boundary conditions, three coefficients each had to be determined. In consequence, u and v had to be joined continuously with continuous first and second derivatives within the boundary layer. This gave six linear homogeneous equations for the six still indeterminate coefficients and the stipulated disappearance of the six-row determinant of this equation system produced the conditional equation between μ, σ, and τ. But these calculations failed at the evaluation of the determinants. The values of u and v to be gained from the series and their derivatives could still be determined with an accuracy of 1 percent at $\eta = 0.5$, but on account of the unavoidable large figures appearing in the solution of the determinants, the

results could no longer be regarded as reliable. On the other hand, near the minimum on the curve of $\dfrac{U_0\delta}{\nu}\sqrt{\dfrac{\delta}{R}}$ against $\alpha\delta$, they yielded results which in order of magnitude agreed with the previous calculations. Because of the surprisingly small values of the critical Reynolds number, the new calculations explained above were carried out.

The next step was to find the extent of the change in the results by a different choice of basic flow $U(\eta)$. To this end the calculations with the $\eta^{(k)}$ places 0, 1/4, 1/2, 3/4, 1 were repeated for the boundary-layer profiles

$$U(\eta) = \begin{cases} \left(\sin\dfrac{\pi}{2}\dfrac{\eta+\epsilon}{1+\epsilon} - \sin\dfrac{\pi}{2}\dfrac{\epsilon}{1+\epsilon}\right)\left(1 - \sin\dfrac{\pi}{2}\dfrac{\epsilon}{1+\epsilon}\right)^{-1} \\[2mm] \qquad\text{for } 0 \leqq \eta \leqq 1 \\[2mm] \qquad 1 \text{ for } \eta \geqq 1 \end{cases} \qquad (5.1)$$

with $\dfrac{\pi}{2}\dfrac{\epsilon}{1+\epsilon} = \pm 1$, that is, $\epsilon_1 = 1.752$, $\epsilon_2 = -0.3890$. The first profile ($\epsilon = 1$) has negative curvature throughout, the second, ($\epsilon = \epsilon_2$) has an inversion point. (See fig. 5, curves (2) and (3).)

To assure a physically logical comparison of the results for the several boundary-layer profiles, it was postulated that all profiles have the same momentum thickness

$$\vartheta = \dfrac{1}{U_0{}^2}\int_0^\delta (U_0 - u_0)u_0\,dy = \delta\int_0^1 (1 - U)U\,d\eta \qquad (5.2)$$

which is a measure for the loss of momentum in the boundary layer. This condition is met when between the individual boundary-layer thicknesses the relation $\vartheta = 0.111\delta = 0.132\delta_1 = 0.137\delta_2$ exists. Here δ denotes the previously defined thickness of the Blasius plate boundary layer, δ_1 and δ_2 the boundary-layer thickness ($\eta = 1$) for the sine profiles (5.1) with ϵ_1 and ϵ_2.

The result of the comparison is shown in figure 6. It was found that, when $\dfrac{U_0\vartheta}{\nu}\sqrt{\dfrac{\vartheta}{R}}$ is plotted against $\alpha\vartheta$, the individual curves within

the scope of our approximation do not differ appreciably from one another. (A corresponding comparison based on the displacement thickness δ^* instead of ϑ produces curves which differ from one another considerably.)

A final calculation, as the roughest approximation to an actual boundary-layer profile, was made on the section profile

$$U = \left\{ \begin{array}{l} \eta \text{ for } 0 \leqq \eta \leqq 1 \\ 1 \text{ for } \eta \geq 1 \end{array} \right\} \tag{5.3}$$

(compare curve 4, fig. 5). If δ_3 is the boundary-layer thickness of this profile ($y = \delta_3$ at $\eta = 1$), then $\vartheta = \frac{1}{6} \delta_3$. At identical momentum thickness with that of the profiles used so far, the difference is slightly greater, but, considering the rough approximation (5.3), the departure from the results so far is not very great. (Compare curve 4, fig. 6.)

The amplifications in the explored wave-length range, at least in vicinity of the critical Reynolds numbers, can be determined by the same approximate method. These calculations were made on the Blasius plate boundary-layer profile. Instead of the extreme case (3.1a) of Green's function $H(\eta; \eta_0)$, the more general expression is obtained from (3.1). To each $\alpha\delta$ and $\frac{\beta\delta^2}{\nu}$, that is, to each pair of parameters σ, τ, there corresponds a particular value of the dimensionless $\frac{U_0 \delta}{\nu} \sqrt{\frac{\delta}{R}}$. The curves $\frac{\beta\vartheta^2}{\nu} = \text{Constant}$ are obtained by graphical interpolation after conversion of δ to ϑ. (Compare fig. 8.) For greater parameter values $\frac{\beta\vartheta^2}{\nu}$, the quality of the approximate calculation decreases quickly.

6. ASYMPTOTIC STATEMENTS

Supplemental to these results for great and small values of $\alpha\delta$, a few statements are indicated. A differential equation of the sixth order for u alone can be obtained from (2.7) by elimination of v. Its form is disagreeable for the general calculation, but it enables a prediction to be made for the extreme cases of great and small values of σ and τ. In this differential equation the coefficients relative to σ and τ represent polynomials up to the sixth degree. Considering only the two highest powers on the assumption of sufficiently great values of σ and τ inside the boundary layer, the problem reduces to the second

order differential equation

$$\tau^2(2\sigma^2 + \tau^2)U'^2u'' - 2\tau^2(\sigma^2 + \tau^2)U'U''u' +$$

$$\left\{\tau^2(\sigma^2 + \tau^2)(2U''^2 - U'U''') - \sigma^2\tau^4U'^2\right\}u = -\mu UU'^3u \qquad (6.1)$$

Integration of this equation across the boundary layer gives the relation

$$\frac{U_0\delta}{\nu}^2\frac{\delta}{R} = \frac{\int_0^1 \left[\left\{\sigma^2\tau^4U'^2 - \tau(\sigma^2 + \tau^2)(2U''^2 - U'U''')\right\}u + 2\tau^2(\sigma^2 + \tau^2)U'U''u' - \tau^2(2\sigma^2 + \tau^2)U'^2u''\right]d\eta}{2\sigma^2\int_0^1 UU'^3ud\eta} \qquad (6.2)$$

The integrals still contain the unknown function u and its first and second derivative, but the derivatives multiplied by polynomials of lower degree in σ, τ, so that the essential contributions to the integral are already included in the estimation

$$\left(\frac{U_0\delta}{\nu}\right)^2\frac{\delta}{R} = \frac{\tau^4}{2}\frac{\int_0^1 U'^2ud\eta}{\int_0^1 UU'^3ud\eta} \qquad (6.2a)$$

Equation (6.2a) is evaluated by an approximation expression for u by means of a polynomial of the fourth degree in η, taking into consideration the boundary conditions $u(0) = 0$, $u''(0) = 0$ (hence $v(0) = 0$), $u'''(0) - \tau^2u'(0) = 0$ (hence $w(0) = 0$) and $u'(1) + \tau u(1) = 0$ (constant connection with constant tangent to the solution for u outside the boundary layer, which according to (2.7) is given by $u = $ Constant $e^{-\tau\eta}$ on account of $U'(\eta) = 0$ for $\eta \geqq 1$ and hence $u'' - \tau^2u = 0$). As a result u is closely approximated in wall proximity and the postulated decay toward the outside is attained. Minor errors in u near the outer edge of the boundary layer are of no consequence in view of the rapidly decreasing U'; errors of u in the numerator and denominator act in the same direction (positive integrands throughout), thus affecting the result very little. Again the asymptotic relation (6.2a) manifests the existence of instability at concave walls only $(R > 0)$.

The defined polynomial for u reads rigorously

$$u = \text{constant}\left\{(\tau + 4)\eta + \tau^2(\tau + 4)\frac{\eta^3}{3!} - \left(1 + \tau + \frac{\tau^2}{2} + \frac{\tau^3}{3!}\right)\eta^4\right\} \qquad (6.3)$$

but in practice only the highest powers of τ are effective for great τ. Figure 7 represents this approximate function u for several values of τ.

The evaluation of the above appraisal for very great σ and τ gives for the Blasius plate profile the asymptotic formula

$$\frac{U_0\vartheta}{\nu}\sqrt{\frac{\vartheta}{R}} \approx 2,3\left(\alpha^2\vartheta^2 + \frac{\beta\vartheta^2}{\nu}\right) \tag{6.4}$$

corrected for ϑ.

The same calculation for the section profile (5.3) gives the factor 2.1 instead of 2.3, hence, a slight difference only. The tie-in with the results obtained for average σ values is readily accomplished with the asymptotic formula (6.4). Figure 8 represents the variation of the critical factor $\frac{U_0\vartheta}{\nu}\sqrt{\frac{\vartheta}{R}}$ plotted against $\alpha\vartheta$ in the double logarithmic net (curve $\frac{\beta\vartheta^2}{\nu} = 0$). The first amplification curves $\frac{\beta\vartheta^2}{\nu} = c = $ Constant > 0 are also shown. The variation of these curves at high $\alpha\vartheta$ values is obtained by addition of 2.3c to the critical values of $\frac{U_0\vartheta}{\nu}\sqrt{\frac{\vartheta}{R}}$ at equal $\alpha\vartheta$, as is readily apparent from (6.4). Moreover, by (6.4)

$$\frac{\beta\vartheta}{U_0} = 0.43\sqrt{\frac{\vartheta}{R}} - \frac{\alpha^2\vartheta^2}{U_0\vartheta/\nu} \leqq 0.43\sqrt{\frac{\vartheta}{R}} \tag{6.5}$$

at great $\alpha\vartheta$, which constitutes an upper limit for the dimensionless amplification quantity $\frac{\beta\vartheta}{U_0}$ solely dependent on $\frac{\vartheta}{R}$.

An asymptotic prediction for small σ is obtained also by an appropriate analysis. It is found that the critical factor $\frac{U_0\vartheta}{\nu}\sqrt{\frac{\vartheta}{R}}$ increases proportional to $(\alpha\vartheta)^{-1}$ with decreasing $\alpha\vartheta$, as expressed in figure 8. (For a more accurate prediction, data about the sixth derivative of u and v are necessary.)

7. DISCUSSION OF THE RESULTS

On the basis of the data collected in the foregoing, the questions formulated above can now be answered in some detail. As regards the

stability limit, that is, the Reynolds number at which vortices of the particular type can exist for the first time without decaying again, is

$$\frac{U_0 \vartheta}{\nu} \approx 0.58 \sqrt{\frac{R}{\vartheta}} \qquad \left(\frac{U_0 \delta}{\nu} \approx 16 \sqrt{\frac{R}{\delta}} \right) \qquad (7.1)$$

It involves vortices at which $\alpha \vartheta \approx 0.14$, that is, whose wave length λ is given by

$$\lambda \approx 45\vartheta (= 5.0\delta) \qquad (7.2)$$

For the Taylor vortices between stationary outside and rotating inside cylinder (ref. 3), the vortex appearing at the stability limit has a wave length of about double the distance of the two cylinders, the vortices thus filling quadratic cells (fig. 1). In the present case they fill cells with a width of about 2-1/2 times the boundary-layer thickness; they even extend beyond the boundary layer. The stability limit for the Taylor vortices is given by $\frac{U_0 \vartheta}{\nu} = 41.3 \sqrt{\frac{R}{d}}$, where d is the cylinder spacing and U_0 the velocity of the rotating inside cylinder while the outside cylinder is at rest. At $\vartheta = \frac{1}{6} d$, $\frac{U_0 \vartheta}{\nu} = 2.81 \sqrt{\frac{R}{\vartheta}}$.

The appearance of the first vortices in the boundary layer does in no way indicate incipient turbulence of the flow. On the contrary, it should be emphasized that the flow will be regular in every way, just the same as before. (Naturally, it does not include the case in which ordinary plate turbulence already occurs at very great $\frac{R}{\delta}$.) No incipient turbulence can be produced until the Reynolds numbers become considerably higher so that the disturbances of an entire range of wave lengths experience sufficient amplification. The same holds true for the Taylor vortices between fixed outside and rotating inside cylinder; the vortices first appear as predicted, but the flow does not become turbulent until the velocities are higher.

The theory developed in the present report postulates that the variation of the flow in principal flow direction is small enough to be disregarded. When the variation in x-direction is small, the results obtained retain their validity as good approximations. In consequence it is justified, under this hypothesis, to inquire into the fate of a vortex of given wave length in its wandering in flow direction through a boundary-layer thickening up at constant outside velocity. The momentary shape of the boundary layer has no appreciable effect on the results, as already seen, when it is referred to the momentum thickness as characteristic length.

In the $\left(\dfrac{U_0 \vartheta}{\nu} \sqrt{\dfrac{\vartheta}{R}}, \; \alpha\vartheta\right)$ diagram the vortices of constant wave length λ describe, by virtue of the identity

$$\frac{U_0 \vartheta}{\nu} \sqrt{\frac{\vartheta}{R}} = (2\pi)^{-3/2} \frac{U_0 \lambda}{\nu} \sqrt{\frac{\lambda}{R}} \; (\alpha\vartheta)^{3/2} \tag{7.3}$$

curves of the configuration

$$\frac{U_0 \vartheta}{\nu} \sqrt{\frac{\vartheta}{R}} = C \; (\alpha\vartheta)^{3/2} \tag{7.4}$$

with $(2\pi)^{3/2} \; C = \dfrac{U_0 \lambda}{\nu} \sqrt{\dfrac{\lambda}{R}} =$ Constant. These curves cross the system of curves of constant amplification and are reproduced for some values of the parameter $\dfrac{U_0 \lambda}{\nu} \sqrt{\dfrac{\lambda}{R}}$ in figure 8. There are curves in this series which cross the zone of unstable disturbances - when they enter it they always cross it since the curves of constant amplification, and especially the curve $\dfrac{\beta \vartheta^2}{\nu} = 0$ at great α values, vary proportional to $(\alpha\vartheta)^2$ (see equation (6.4)) - and there are curves in the series that never reach the instability range. Thus, the vortices corresponding to the latter are never amplified but always swallowed by the viscosity effect. In the extreme case there is a curve which is tangent to the neutral curve $\dfrac{\beta \vartheta^2}{\nu} = 0$. This is the case for the curve with the parameter $\dfrac{U_0 \lambda}{\nu} \sqrt{\dfrac{\lambda}{R}} = 50$ shown in figure 8. Therefore, if the disturbance of the wave length in wandering through the thickening boundary layer ever is to reach an undamped state, $\dfrac{U_0 \lambda}{\nu} \sqrt{\dfrac{\lambda}{R}}$ must be $\geqq 50$; that is, the inequality

$$\frac{\lambda}{R} \geqq 13.6 \left(\frac{U_0 R}{\nu}\right)^{-2/3} \tag{7.5}$$

must be fulfilled, which affords a measure for the smallest vortices which are able to experience amplification at all. At the instant where it reaches its solitary neutral state, the particular boundary disturbance has a specific wave length referred to the momentum thickness prevailing at that point. According to figure 8, the contact of the aforementioned curves occurs at about $\alpha\vartheta \approx 1.1$, where, therefore,

$$\lambda \approx 5.7\vartheta = 0.63\delta \tag{7.6}$$

Therefore, the wave length λ of the disturbance must have a certain magnitude characterized by (7.5) if it ever is to get in a critical situation with the increasing boundary-layer thickness. If equality exists in (7.5), this instant is given by the fulfillment of (7.6); damping occurs before and after. If inequality exists in (7.5), then the critical ratio of wave length to boundary-layer thickness is already reached at a certain stage, where as yet $\frac{\lambda}{\delta} > 0.63$, after which the disturbance is amplified until a certain second ratio $\frac{\lambda}{\delta} < 0.63$ is reached; from then on the disturbance is damped again. However, the prediction about the second critical ratio is applicable only when the disturbance on the previously transversed path of amplification does not exceed the theoretically specified range of "small" disturbances.

The last question to be answered concerns the most dangerous disturbances, that is, disturbances in the whole range of wave lengths which in traveling through the boundary layer at equal Reynolds number $\frac{U_0 \vartheta}{\nu}$ experience the highest amplification, or in figure 8, the curves $\frac{U_0 \lambda}{\nu}\sqrt{\frac{\lambda}{R}}$ = Constant, which prevail at the start of their amplification path before transition to turbulent flow in the range of minimums of the curves $\frac{\beta \vartheta^2}{\nu}$ = Constant.

In an article by M. and F. Clauser (ref. 9), the appearance of turbulent flow at the concave wall was observed for $Re_x = \frac{U_0 x}{\nu} = 2.6 \times 10^5$ at point $\frac{x}{R} = 0.75$ and for $Re_x = 3.1 \times 10^5$ at point $\frac{x}{R} = 0.45$. Using the Blasius law of growth of the boundary layer at the flat plate $\left(\vartheta = \frac{2}{3}\sqrt{\frac{\nu x}{U_0}}\right)$ as basis, the values of the critical dimensionless factor $\frac{U_0 \vartheta}{\nu}\sqrt{\frac{\vartheta}{R}}$ are 10.6 and 8.6. They are indicated by the dashed markings in figure 8. A rough extrapolation indicates that, in the vicinity of these values, the amplification curves $\frac{\beta \vartheta^2}{\nu}$ = Constant $\left(\text{or the curves}\right.$ $\frac{\beta x}{U_0}$ = Constant = $\frac{9}{4}\frac{\beta \vartheta^2}{\nu}$ which, based upon the law $\vartheta = \frac{2}{3}\sqrt{\frac{\nu x}{U_0}}$, is the same$\left.\right)$ are minimum at about $\alpha = 0.6$, hence $\alpha \delta = 5.5$. Assuming that the turbulence is caused by vortices of the type investigated here, at reversal the boundary-layer thickness would, roughly speaking, have increased up to the order of magnitude of the width of the highest amplified vortices. The latter, in turn, would have a wave length λ of about $\lambda \approx 50R\left(\frac{U_0 R}{\nu}\right)^{-2/3}$.

For a more accurate prediction about the most dangerous vortices, the particular total amplification throughout the unstable range would have to be determined for different vortices α = Constant by integration; but for this, the few amplification curves, which at greater values of $\dfrac{\beta \vartheta^2}{\nu}$ become unreliable, is insufficient.

Translated by J. Vanier
National Advisory Committee
for Aeronautics

REFERENCES

1. Blasius, H.: Grenzschichten in Flüssigkeiten mit kleiner Reibung. Diss. Göttingen 1907, erschienen in Z. f. Math. u. Physik, Bd. 56, 1908, pp. 1-37. (Available as NACA TM 1256.)

2. Noether, F.: Das Turbulenzproblem. ZAMM 1, 1921, pp. 125-138.

3. Taylor, G. I.: Stability of Viscous Liquid Contained Between Two Rotating Cylinders. Phil. Trans. Roy. Soc. (London), vol. 223, Feb. 8, 1923, pp. 289-343.

4. Prandtl, L.: Einfluss stabilisierender Kräfte auf die Turbulenz. Vortrage aus dem Gebiet der Aerodynamik und verwandter Gebiete. Aachen 1929, pp. 1-7. (Available as NACA TM 625.)

5. Schlichting, H.: Über die Entstehung der Turbulenz in einem rotierenden Zylinder. Nachr. Ges. Wiss. Göttingen, Math.-Phys. Kl. 1932, pp. 160-198.

6. Squire, H. B.: Stability for Three-Dimensional Disturbances of Viscous Fluid Flow Between Parallel Walls. Proc. Roy. Soc. (London), ser. A, vol. 142, Nov. 1, 1933, pp. 621-628.

7. Schlichting, H.: Neuere Untersuchungen über die Turbulenzentstehung. Naturwissenschaften, 22. Jahrg, 1934, pp. 376-381.

8. Prandtl, L.: The Mechanics of Viscous Fluids. Vol. III of Aerodynamic Theory, div. G, W. F. Durand, ed., Julius Springer (Berlin), 1935, pp. 34-208.

9. Clauser, Milton, and Clauser, Francis: The Effect of Curvature on the Transition From Laminar to Turbulent Boundary Layer. NACA TN 613, 1937.

10. Görtler, H.: Über den Einfluss der Wandkrümmung auf die Entstehung der Turbulenz. Z.f.a.M.M., Bd. 20, Heft 3, June 1940, pp. 138-147.
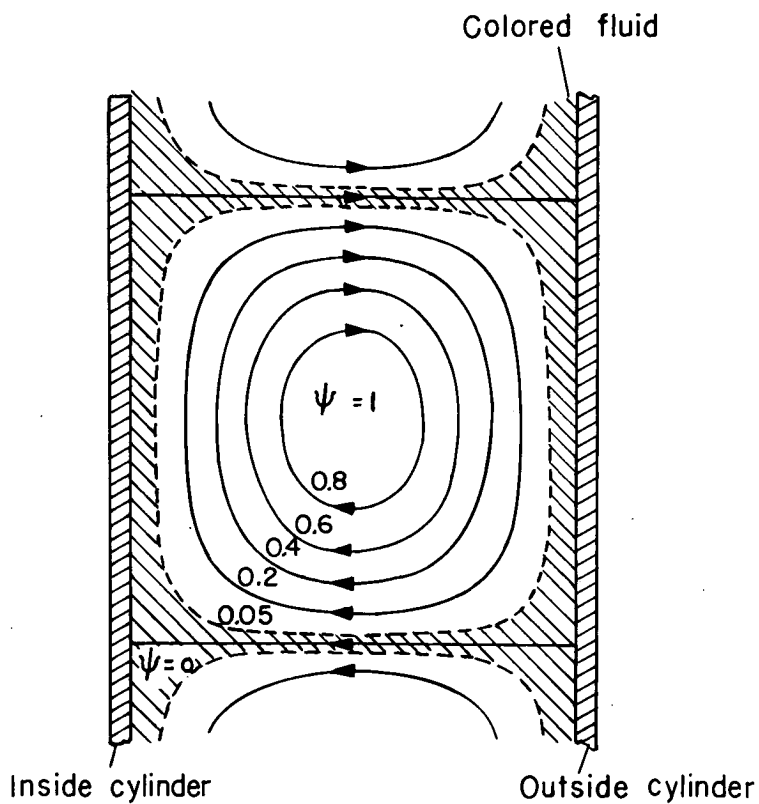
Figure 1.- Vortex between the walls of two concentric rotating
cylinders according to G. I. Taylor, streamline pattern following
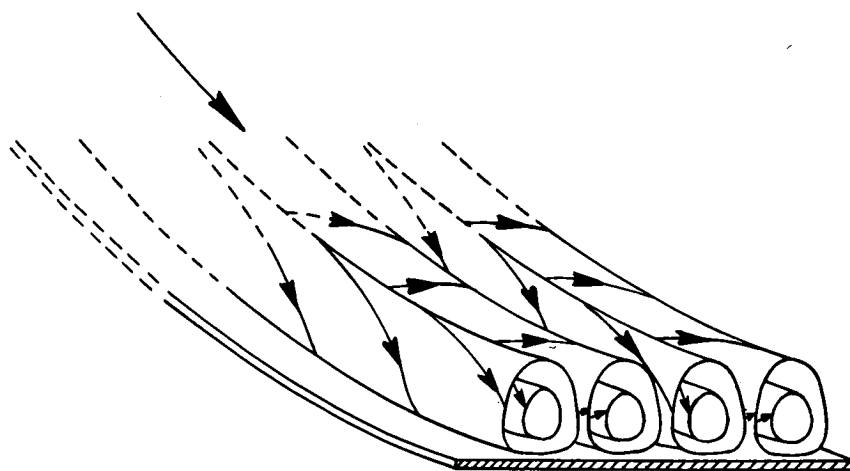incipient instability (inside and outside cylinder rotate in same
direction).

Figure 2.- Vortex disturbances in the flow of a fluid on a concave wall,
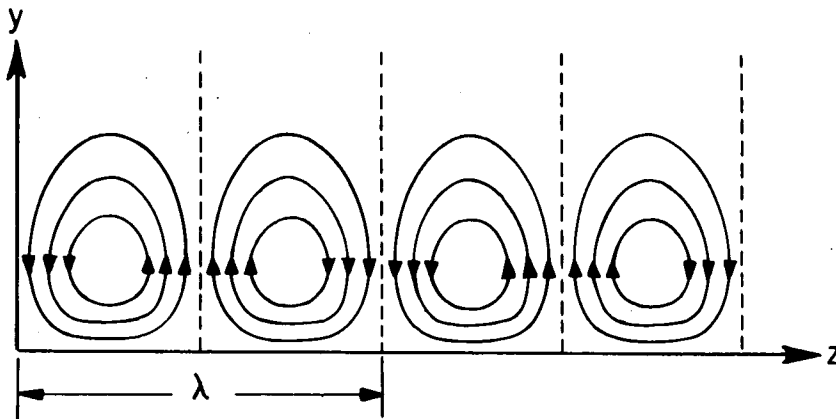axes of vortices parallel to principal flow direction.

Figure 3.- Scheme of streamline pattern in a section at right angle to
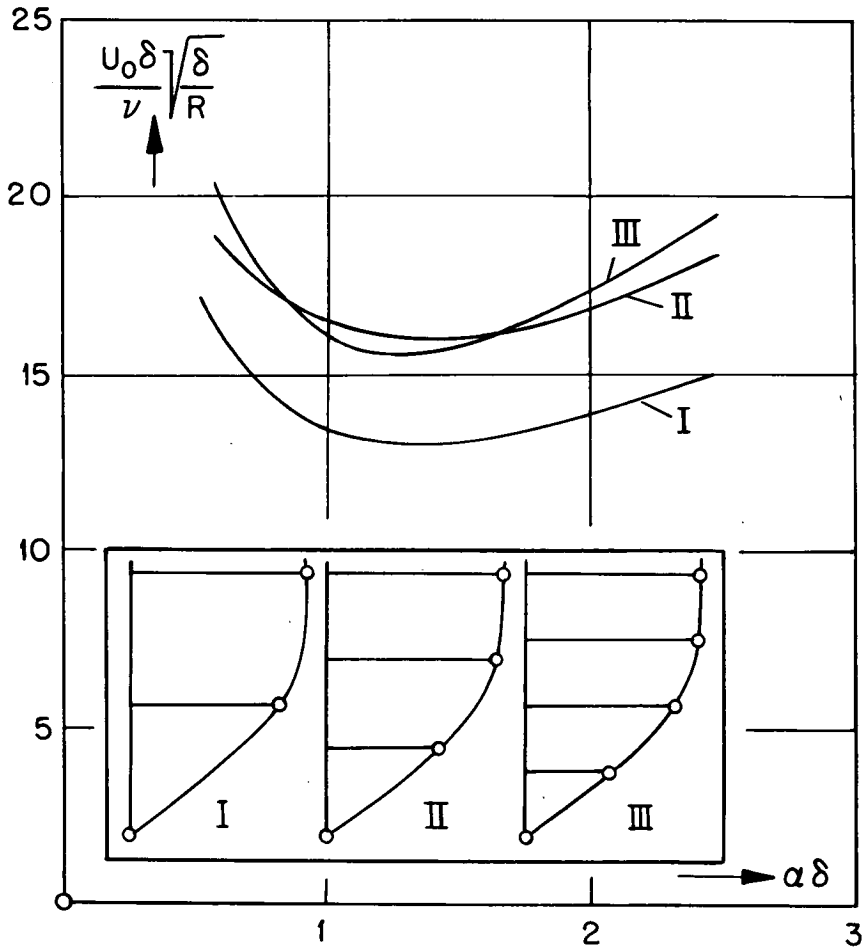the principal flow direction.

Figure 4.- The critical factor $\dfrac{U_0\delta}{\nu}\sqrt{\dfrac{\delta}{R}}$ for Blasius's flat plate bound-

ary layer plotted against $\alpha\delta$ computed by three increasing
approximations.
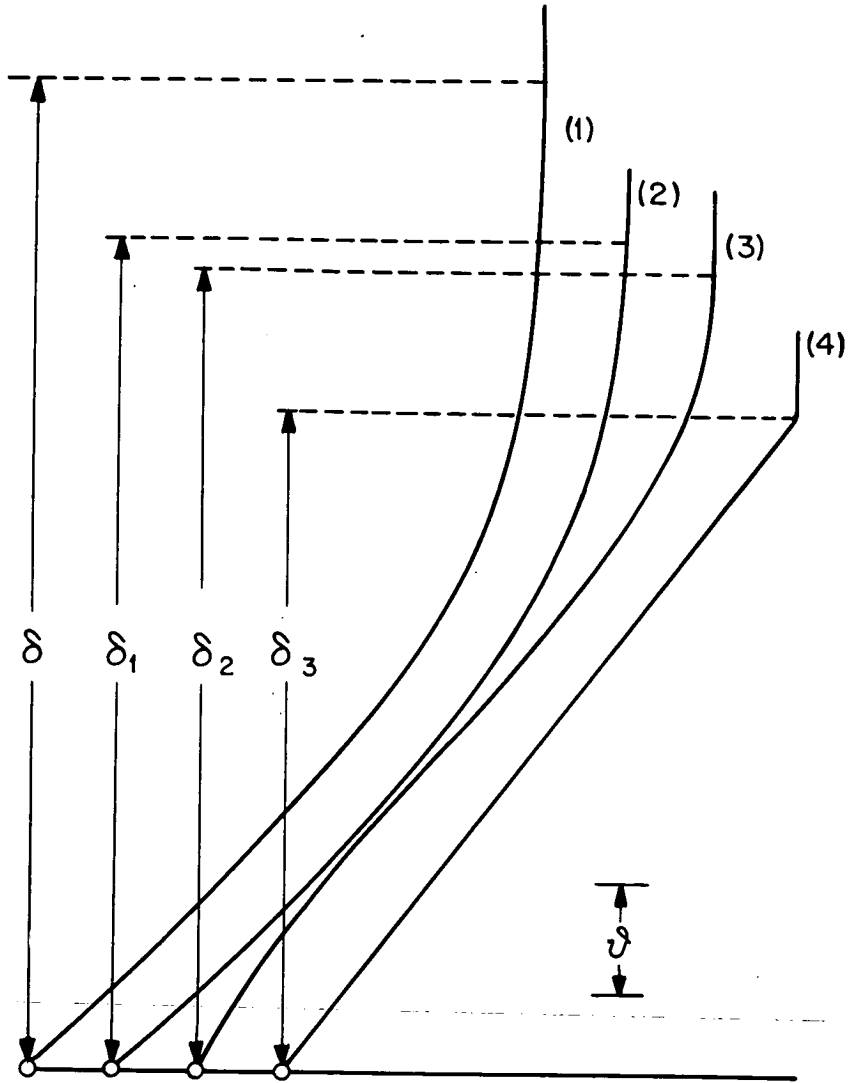
Figure 5.- The boundary-layer profiles of equal momentum thickness ϑ used as basis of the calculation.
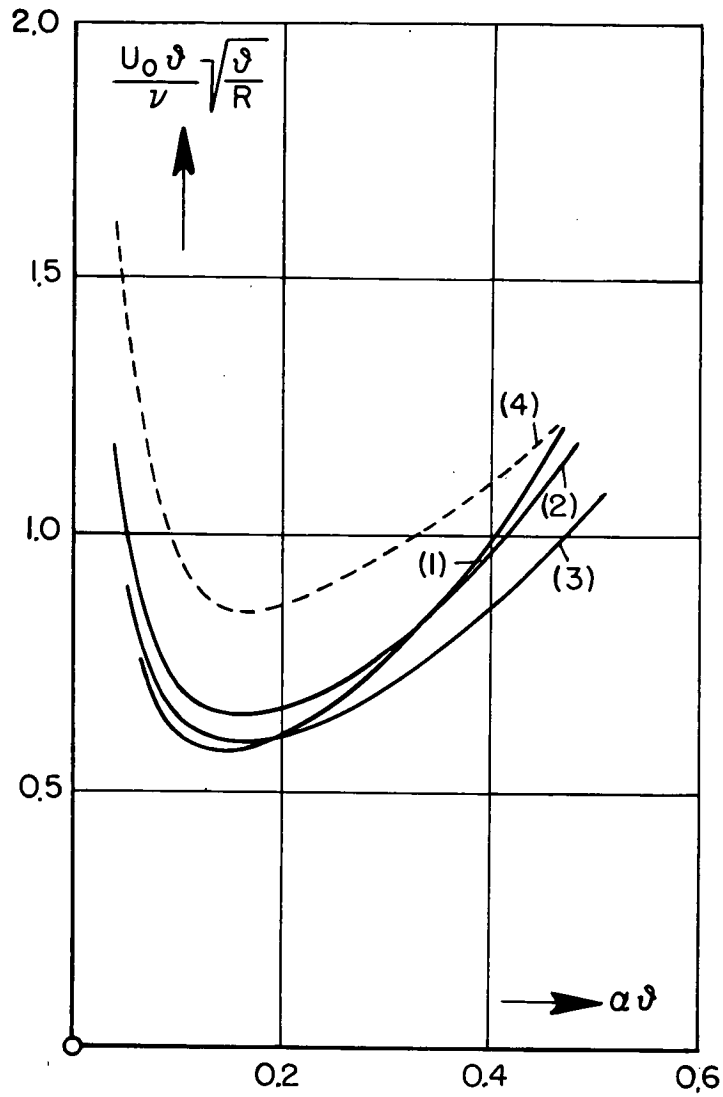
Figure 6.- The critical factor $\dfrac{U_0\vartheta}{\nu}\sqrt{\dfrac{\vartheta}{R}}$ plotted against $\alpha\vartheta$ for the boundary-layer profiles of figure 5.
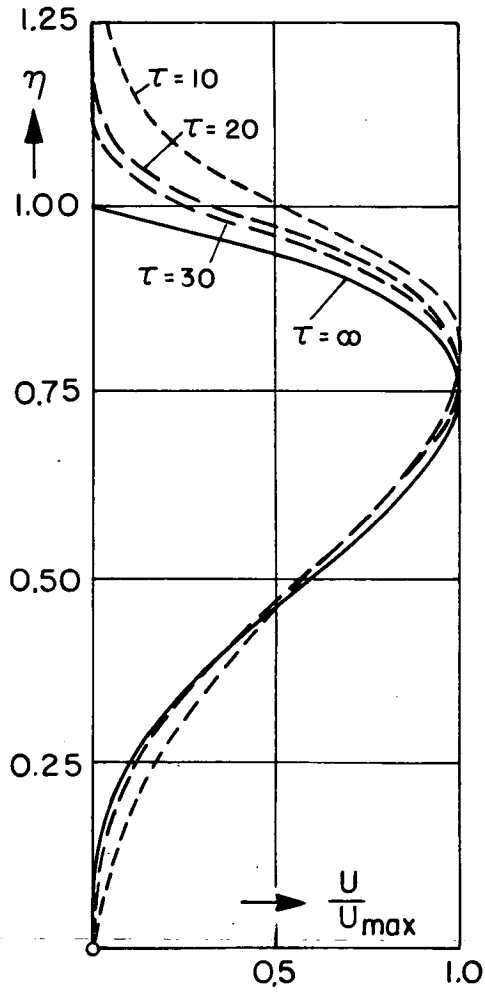
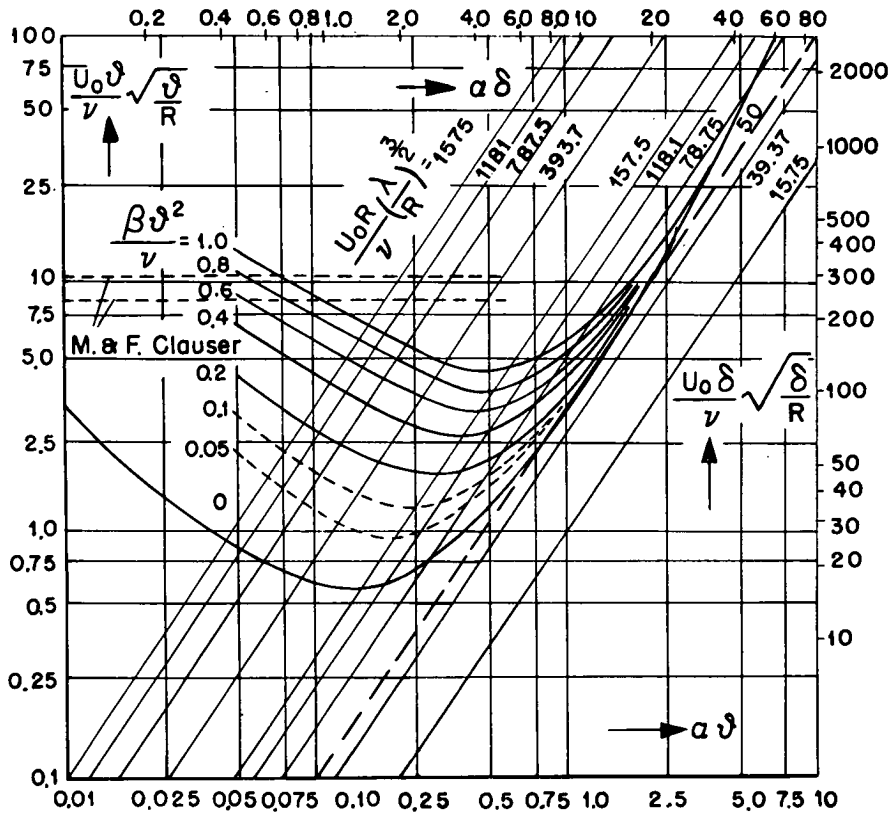Figure 7.- Approximate function for u (according to equation (6.3)).

Figure 8.- Total variation of the critical factor $\dfrac{U_0 \vartheta}{\nu}\sqrt{\dfrac{\vartheta}{R}}$ plotted against $\alpha\vartheta$ and the first amplification curves $\dfrac{\beta\vartheta^2}{\nu} = $ const. The parallel lines in this diagram represent individual vortices (λ = const.) in a slowly thickened boundary layer at constant outside flow velocity U_0.